You *et al. PhotoniX* (2024) 5:39
https://doi.org/10.1186/s43074-024-00153-4

PhotoniX

RESEARCH Open Access

Isolating the classical and quantum coherence of a multiphoton system

Chenglong You[1*], Mingyuan Hong[1], Fatemeh Mostafavi[1], Jannatul Ferdous[1], Roberto de J. León-Montiel[2], Riley B. Dawkins[1] and Omar S. Magaña-Loaiza[1]

*Correspondence: cyou2@lsu.edu

[1] Quantum Photonics Laboratory, Department of Physics & Astronomy, Baton Rouge 70803, LA, USA
[2] Instituto de Ciencias Nucleares, Universidad Nacional Autónoma de México, Apartado Postal 70-543, 04510 Ciudad de México, México

Abstract

The classical properties of thermal light fields were instrumental in shaping our early understanding of light. Before the invention of the laser, thermal light was used to investigate the wave-particle duality of light. The subsequent formulation of the quantum theory of electromagnetic radiation later confirmed the classical nature of thermal light fields. Here, we fragment a pseudothermal field into its multiparticle constituents to demonstrate that it can host multiphoton dynamics mediated by either classical or quantum properties of coherence. This is shown in a forty-particle system through a process of scattering mediated by twisted paths endowed with orbital angular momentum. This platform enables accurate projections of the scattered pseudothermal system into isolated multiphoton subsystems governed by quantum dynamics. Interestingly, the isolated multiphoton subsystems exhibiting quantum coherence produce interference patterns previously attributed to entangled optical systems. As such, our work unveils novel mechanisms to isolate quantum systems from classical fields. This possibility opens new paradigms in quantum physics with enormous implications for the development of robust quantum technologies.

Keywords: Many-body system, Quantum statistics, Quantum coherence, Photon-number-resolving detection

Introduction

Ever since the birth of quantum physics, there has been a growing interest in the identification of the boundary between the classical and quantum worlds [1–3]. Over the past decades, the investigation of quantum many-body systems has facilitated seminal studies that aim to uncover the nonclassical properties of macroscopic systems [2, 3]. The verification of quantum superpositions, wave-particle duality, entanglement, and decoherence of multiparticle systems has provided some insights on this matter [2–9]. These studies have shown that quantum multiparticle systems can host many complex forms of interference and scattering processes that are essential to perform operations that are intractable on classical systems [10–12]. Recently, the fundamental physics and technological potential of large multiparticle systems have stimulated the engineering of diverse platforms for their preparation [2, 12, 13]. Typical

platforms include trapped atoms, quantum dots, superconducting qubits, nitrogen-vacancy centers, and photonic systems [2, 13]. Due to the remarkable properties of photons to exhibit quantum properties at room temperature, large quantum photonic systems constitute a promising platform for the investigation of many-body systems [12, 14, 15].

Here we isolate the quantum many-body components within a classical pseudothermal optical system [12, 15–18]. While most of the isolated multiphoton subsystems exhibit classical coherence properties and interference dynamics similar to those of the hosting pseudothermal system, a subset reveals striking quantum coherence properties that contrast with the behavior of that hosting system. In our work, we extract multiphoton quantum subsystems by performing projective measurements of the particle number of a classical optical system [14, 19, 20]. This measurement scheme enables us to observe the quantum coherence of many-body subsystems with up to forty interacting particles. Specifically, we explore the distinctive roles of classical and quantum coherence by measuring multiparticle dynamics of vortices produced by the interference of random classical light waves [21–24]. Interestingly, we demonstrate that the extracted many-body systems exhibiting anti-coalescence effects induce correlated interactions. Furthermore, we found that those multiparticle subsystems exhibiting coalescence produce anti-correlated dynamics, which are opposite to the macroscopic behavior of the hosting pseudothermal system [25]. Remarkably, the potential to isolate quantum coherence within classical open systems not only holds fundamental significance for quantum physics but also presents profound implications for retrieving the quantum features of open physical systems affected by decoherence processes [26–29].

Results

The formation of dislocations in incoherent random waves has sparked significant interest in the investigation of vortices in diverse physical systems [21–23, 30–32]. In this work, we prepared a classical random optical system with many transverse spatial singularities [17]. This is shown in the first panel of Fig. 1a, where we plot the spatial intensity distrubtion of our system. This classical system hosts many-body quantum subsystems whose vortex dynamics are nonclassical and cannot be described using Berry's formalism [21, 23, 31]. Remarkably, the constituent many-body subsystems within the classical random system unveil different spatial structures with distinct transverse vortex distributions. We extract multiphoton quantum subsystems by performing projective measurements on Fock states [33]. As described below, these measurements enable us to collapse the state of the scattered macroscopic system onto isolated multiphoton subsystems [26]. Interestingly, the extracted probability distribution of the multiparticle subsystems reported in Fig. 1a exhibit peculiar vortex dynamics. The presence of these vortices imprints an orbital angular momentum (OAM) spectrum onto our macroscopic system [23, 24]. Here, we characterize its vortex dynamics by analyzing the OAM correlations of its constituent multiparticle subsystems. This can be achieved by expressing the inital pseudothermal light field through the following OAM-dependent density matrix in the Fock state basis, which we have here written in the coherent-state basis for simplicity as

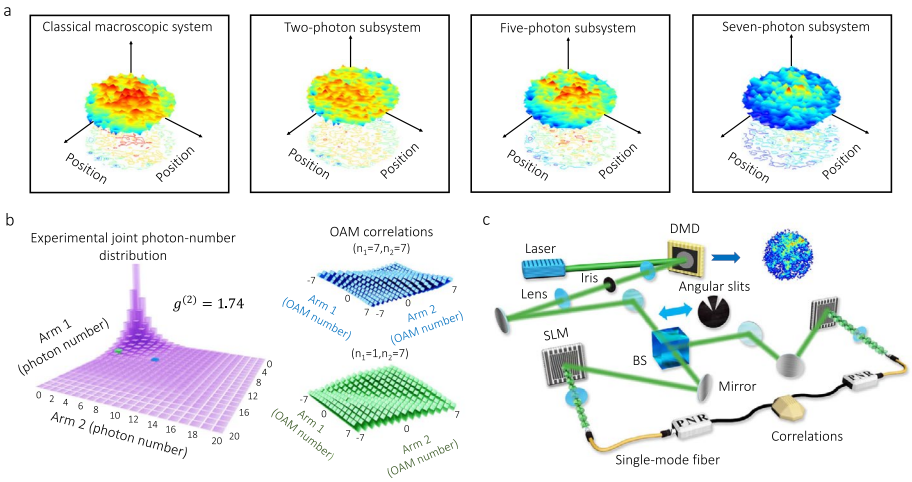

Fig. 1 Classical optical system and its constituent quantum many-body subsystems. The classical light field in our experiment consists of a random optical field with transverse spatial singularities [21, 30]. This is reported in the first panel of (**a**). Interestingly, the pseudothermal light field hosts many-body quantum subsystems with different distributions of vortices. Our experimental measurement of the spatial distribution of the many-body subsystems is reported in the other panels of (**a**). We extract the quantum multiparticle subsystems from the pseudothermal light field by implementing projective measurements on Fock states [26]. In panel (**b**), we report the experimentally measured joint photon-number distribution of our classical light field. This shows our capability to isolate many-body quantum subsystems with up to forty particles. The degree of second-order coherence $g^{(2)}$ for the classical system is 1.74, which corresponds to the degree of coherence of a classical light beam [34]. The OAM correlations for two projected many-body subsystems consisting of eight and fourteen particles are shown in the right part of (**b**). These correlations are measured using the setup depicted in (**c**). Here we use a digital micromirror device (DMD) to produce a pseudothermal light field containing multiple independent wavepackets with randomly modulated phases [16, 17]. We pass the beam through a beam splitter to measure its correlation properties. We add an angular double slit to study its quantum multiparticle dynamics. The beams reflected by the spatial light modulators (SLMs) are projected onto specific OAM values and then measured by two superconducting nanowire single-photon detectors that are used to perform photon-number-resolving (PNR) detection [14, 19, 20]. Our experiment is finalized by correlating the signals from the detectors (see Materials and methods section). This kind of measurement enables the isolation of specific quantum dynamics

$$\hat{\rho}_{\ell_1,\ell_2} = \int d^2\alpha d^2\beta P_{\ell_1,\ell_2}(\alpha,\beta)|\alpha,\beta\rangle\langle\alpha,\beta|, \tag{1}$$

where

$$P_{\ell_1,\ell_2}(\alpha,\beta) = \frac{1}{4\pi^2\left|\sigma_{\ell_1}\sigma_{\ell_2} - |\eta_{\ell_1,\ell_2}|^2\right|} \times \exp\left[-\frac{\sigma_{\ell_2}|\alpha-\mu_{\ell_1}|^2 + \sigma_{\ell_1}|\beta-\mu_{\ell_2}|^2 - 2\mathrm{Re}\left[(\alpha^*-\mu_{\ell_1}^*)(\beta-\mu_{\ell_2})\eta_{\ell_1,\ell_2}\right]}{2(\sigma_{\ell_1}\sigma_{\ell_2} - |\eta_{\ell_1,\ell_2}|^2)}\right]. \tag{2}$$

The function $P_{\ell_1,\ell_2}(\alpha,\beta)$ is a complex-Gaussian probability density function for our classical random optical system [35]. Here, α and β are the coherent amplitudes of the two OAM modes ℓ_1 and ℓ_2. Furthermore, the average electric-field amplitudes are represented by μ_{ℓ_i}, and σ_{ℓ_i} and η_{ℓ_i,ℓ_j} are the respective variances and covariances of these electric-field amplitudes. More detailed information can be found in the supplementary information (SI).

Our classical pseudothermal light field, described by Eqs. (1) and (2), hosts many multiparticle quantum systems. In Fig. 1b, we report the experimental joint photon-number distribution of our system hosting many-body subsystems with up to forty photons. Given the classical nature of our random optical field, this can be fully described using Maxwell's equations [24, 30, 34]. The differences among the spatial structures of the multiparticle subsystems in Fig. 1a produce distinct OAM correlations. As shown in Fig. 1b, the strength and nature of these correlations are defined by the isolated many-body quantum subsystem [36]. The origin of these correlations is described below, and these measurements were performed using the experimental setup shown in Fig. 1c. This setup allowed us to measure OAM correlations for the multiparticle subsystems within the random optical system (see Materials and methods section for details). The use of photon-number-resolving (PNR) detection enabled us to collapse the state of the scattered random optical system into isolated multiparticle subsystems that exhibit different quantum dynamics [20, 26]. The projection of the classical pseudothermal system into isolated subsystems unveils peculiar quantum dynamics which can be opposite to the classical dynamics of the hosting system [1–3, 37].

We now discuss the coherence properties of the pseudothermal random system and its constituent many-body subsystems. Given the classical nature of our hosting system, some of its properties can be characterized through the measurement of intensity correlations [33, 34]. Specifically, the OAM correlation measurements can be described by projecting our pseudothermal system onto the OAM modes ℓ_1 and ℓ_2. The density matrix in Eq. (1) allows us to express the degree of second-order coherence for our random hosting system as

$$g^{(2)}(\ell_1,\ell_2)=1+\frac{4|\eta_{\ell_1\ell_2}|^2+4\mathrm{Re}\left[\mu^*_{\ell_1}\mu_{\ell_2}\eta_{\ell_1\ell_2}\right]}{(2\sigma_{\ell_1}+|\mu_{\ell_1}|^2)(2\sigma_{\ell_2}+|\mu_{\ell_2}|^2)}. \tag{3}$$

This expression certifies the classicality of the hosting system reported in Fig. 1b. The detailed derivation of Eq. (3) can be found in the SI. Despite the classical nature of our photonic system, we show that this macroscopic behavior results from the collective dynamics of nonclassical many-body subsystems. Notably, one can access their quantum dynamics by projecting the random optical field into its constituent multiparticle subsystems [14, 19, 20]. The coherence of these isolated subsystems can be described through the following coherence function

$$\tilde{g}^{(2)}(\ell_1,\ell_2,n_1,n_2)=\frac{\mathrm{Tr}\left[\hat{\rho}_{\ell_1,\ell_2}|n_1,n_2\rangle\langle n_1,n_2|\right]}{\left(\sum_n \mathrm{Tr}\left[\hat{\rho}_{\ell_1,\ell_2}|n,n_2\rangle\langle n,n_2|\right]\right)\left(\sum_m \mathrm{Tr}\left[\hat{\rho}_{\ell_1,\ell_2}|n_1,m\rangle\langle n_1,m|\right]\right)}. \tag{4}$$

Here, the coherence function $\tilde{g}^{(2)}(\ell_1,\ell_2,n_1,n_2)$ allows identifying the classical or quantum processes of coherence of the multiparticle subsystems that form the hosting random optical field [25, 38]. As shown in Fig. 2a, the properties of coherence $\tilde{g}^{(2)}(n_1,n_2)$ of the extracted subsystems oscillate as the number of particles increase ($n\to\infty$). Despite the many multiparticle subsystems exhibiting quantum coherence, most multiparticle subsystems exhibit classical properties of coherence.

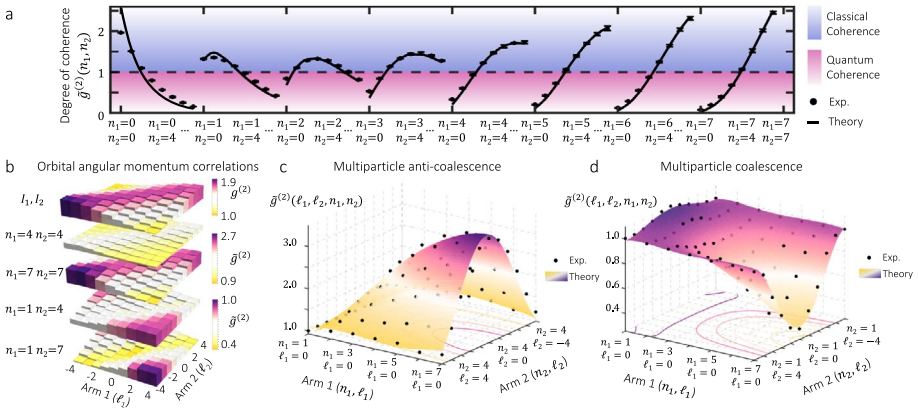

Fig. 2 Classical and quantum coherence of many-body subsystems. As indicated in (**a**), the extracted multiparticle subsystems can exhibit either classical ($\tilde{g}^{(2)}(n_1, n_2) > 1$) or quantum ($\tilde{g}^{(2)}(n_1, n_2) < 1$) properties of coherence. Interestingly, these properties vary with the number of particles in the extracted many-body systems. In this case, we are reporting multiparticle systems that do not carry OAM. Despite the many multiphoton subsystems exhibiting quantum coherence, most of the multiphoton subsystems exhibit classical properties of coherence. Indeed, the quantum dynamics hosted by the pseudothermal light field are overwhelmed by the classical properties of coherence of the majority of the constituent subsystems. The theoretical predictions were calculated based on Eqs. (3) and (4). Furthermore, we report the classical OAM correlations of the random macroscopic system in the first row of (**b**). These correlations are quantified through the second-order coherence function $g^{(2)}(\ell_1, \ell_2)$. The second and third rows therein report similar correlation peaks for symmetric multiparticle subsystems with eight ($n_1 = 4, n_2 = 4$) and fourteen ($n_1 = 7, n_2 = 7$) photons. These correlations are quantified through the coherence function $\tilde{g}^{(2)}(\ell_1, \ell_2, n_1, n_2)$. Remarkably, the fourth and fifth rows in (**b**) demonstrate the existence of OAM-correlation holes for asymmetric subsystems with five ($n_1 = 1, n_2 = 4$) and eight ($n_1 = 1, n_2 = 7$) photons. Interestingly, these processes lead to generalized forms of multiparticle interference that we explore using the angular double-slit structure in Fig. 1c. As reported in (**c**), we observe multiparticle Hanbury Brown and Twiss interference as we scan the OAM of the extracted subsystems with $\tilde{g}^{(2)}(\ell_1, \ell_2, n_1, n_2) > 1$[24]. Notably, the many-body subsystems characterized by $\tilde{g}^{(2)}(\ell_1, \ell_2, n_1, n_2) < 1$exhibit a type of multiparticle Hong-Ou-Mandel effect as shown in (**d**) [39]

Consequently, the quantum dynamics within the pseudothermal system are overshadowed by the classical coherence properties of the majority of the constituent multiphoton subsystems. The contributions from all these isolated subsystems lead to the classical properties of the pseudothermal light beam [24]. Furthermore, the classical OAM correlations of the hosting system are reported in the first row of Fig. 2b. Sharing similarities with the classical system, extracted multiparticle subsystems containing the same number of particles exhibit correlation peaks in their OAM distribution. As indicated by the second and third rows of Fig. 2b, the strength of these correlation peaks scales with the number of particles in the isolated subsystem. Here, the fourteen-particle subsystem ($n_1 = 7, n_2 = 7$) shows stronger OAM correlations than its eight-particle counterpart ($n_1 = 4, n_2 = 4$). Interestingly, the detection of multiphoton subsystems with different numbers of particles in each arm demonstrates the presence of OAM-correlation holes as indicated in the fourth and fifth rows of Fig. 2b. This first observation of correlation holes unveils the presence of quantum coherence governing interactions among certain many-body subsystems that constitute the classical hosting system [25, 38]. Remarkably, multiparticle subsystems characterized with classical properties of coherence ($\tilde{g}^{(2)}(\ell_1, \ell_2, n_1, n_2) > 1$) produce many-body Hanbury Brown and Twiss interference when an angular double-slit structure

is placed in the source [24]. These measurements showing multiparticle anti-coalescence are reported in Fig. 2c. Moreover, the angular double-slit interference of the multiparticle subsystems exhibiting OAM-correlation holes ($\tilde{g}^{(2)}(\ell_1, \ell_2, n_1, n_2) < 1$) produce the multiparticle coalescence reported in Fig. 2d [39]. This effect is mediated by a multiparticle Hong-Ou-Mandel effect in subsystems with up to eleven particles.

We now discuss the implications of multiparticle coalescence and anti-coalescence for the formation of correlated and anti-correlated interference patterns produced by the extracted multiphoton subsystems. These effects can be explored through the scattering of the classical hosting system by the angular double-slit structure shown in Fig. 1c. In this case, we project the scattered multiparticle subsystems in one of the arms into different OAM modes, from $\ell_1 = -15$ to $\ell_1 = 15$, whereas the scattered subsystems in the second arm are projected into $\ell_2 = 3$ (see Materials and methods section for additional information). Given the presence of OAM correlations in classical light [24], the correlations between the two arms lead to the formation of an interference pattern with a peak around $\ell_1 = 3$, as shown in Fig. 3a. As expected, most of the constituent multiphoton subsystems produce interference patterns similar to those of the hosting system. Due to the anti-coalescence effects mediating these interference processes ($\tilde{g}^{(2)}(n_1, n_2) > 1$), the patterns in Fig. 3b also exhibit a peak around $\ell_1 = 3$. Nevertheless, the extracted many-body systems with a larger number of particles produce quantum-enhanced visibilities which surpass that of the classical hosting system. Remarkably, the coalescence

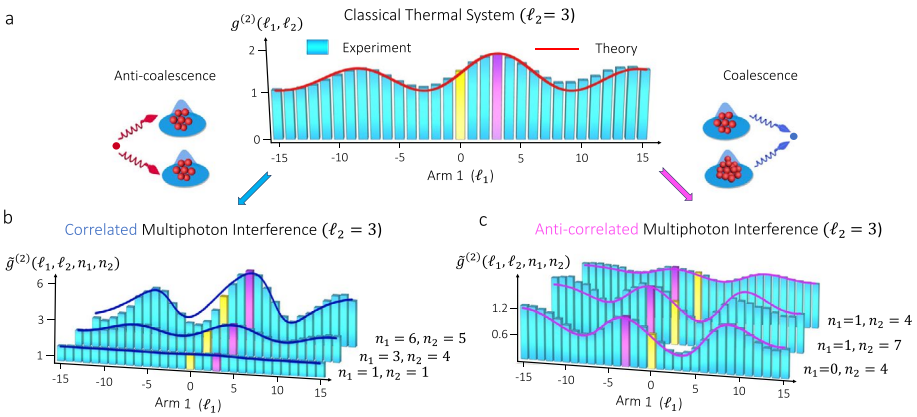

Fig. 3 Observation of correlated and anti-correlatated interference of extracted multiphoton subsystems. The scattering of our random pseudothermal system by a double-slit structure produces the classical interference pattern shown in (**a**). This pattern was obtained by projecting the scattered random field in one of the arms into different OAM modes, from $\ell_1 = -15$ to $\ell_1 = 15$, whereas the scattered photons in the second arm are projected into $\ell_2 = 3$. The separation between the slits is $\pi/6$ radians and their widths are $\pi/12$ radians. The overwhelming presence of multiparticle subsystems with $\tilde{g}^{(2)}(n_1, n_2) > 1$in Fig. 2 induce a correlation shift of three units to the right. These kinds of many-body subsystems exhibiting anti-coalescence dynamics produce other correlated structures with a peak at $\ell_1 = 3$. We report these measurements in (**b**). Interestingly, the visibility of these interference patterns increases with the number of particles in the subsystem, enabling a quantum-enhanced visibility for the many-body subsystem with eleven particles ($n_1 = 6, n_2 = 5$). Despite the direct correspondence between the interference structures in (**a** and **b**), there are quantum processes of coherence inducing the increasing visibilities in (**b**) that surpass that of the classical hosting system in **a**. Remarkably, the projection of the classical pseudothermal system into the many-body subsystems in (**c**) unveils a different interference structure. The coalescence dynamics hosted by these kinds of subsystems, characterized by $\tilde{g}^{(2)}(n_1, n_2) < 1$, produce anti-correlated interference patterns with a peak at $\ell_1 = -3$. Even though the isolated quantum subsystems in (**c**) were extracted from the classical pseudothermal field in (**a**), they exhibit different correlation dynamics

of multiparticle subsystems ($\tilde{g}^{(2)}(n_1, n_2) < 1$) leads to the formation of remarkably different interference structures. Specifically, the extracted multiphoton subsystems produce the anti-correlated interference structures reported in Fig. 3c. Surprisingly, these multiparticle interference patterns reveal a peak at $\ell_1 = -3$. For nearly two decades, this behavior has been attributed to OAM-entangled photons [40], which exhibit OAM anti-correlations due to the conservation of OAM in spontaneous parametric down-conversion processes [41]. Surprisingly, in our experiment, these nonclassical multiphoton subsystems were extracted from a classical optical system. Notably, our theoretical model, which utilizes a complex-Gaussian probability density function, successfully captures all the features observed in our experiment.

Discussions

While extensive research has been devoted to investigating the nonclassical properties of macroscopic quantum systems [1–9], this work provides the first direct evidence of the quantum signatures of the classical world. Our measurements of the quantum dynamics of a classical system demonstrate the contrasting nature between the so-called classical and quantum worlds [1–10, 13, 37, 42]. Our observations reveal the dramatic role that classical and quantum coherence has in the behavior of multiparticle systems. This was demonstrated through a process of multiparticle scattering mediated by twisted paths endowed with orbital angular momentum. The flexibility of our platform enabled us to isolate quantum and classical processes of coherence by performing measurements of the orbital angular momentum and the particle number of multiphoton wavepackets containing up to forty particles. The identification of different coherence conditions allowed us to observe the occurrence of correlated and anti-correlated processes of scattering among the multiphoton wavepackets that form a classical photonic system. Furthermore, our work outlines novel mechanisms to extract and isolate quantum systems from open classical systems [26, 27]. This possibility opens new paradigms in quantum physics with enormous implications for the development of robust quantum technologies [27]. We believe that our discoveries unveil universal properties of many-body systems that are relevant for diverse fields ranging from condensed matter to nuclear physics [2, 10, 13, 43].

Materials and methods

Source preparation

As shown in Fig. 1c, we utilized a continuous-wave laser operating at a wavelength of 532 nm. The initial beam is spatially cleaned and expanded using a 4-f system to match the size of the digital micromirror device (DMD, DLP LightCrafter 6500 Evaluation Module). In our experiment, we generate a pseudothermal light beam with engineered photon statistics. To experimentally generate pseudothermal multiphoton states, we dynamically modulate the laser beam's spatial properties of coherence by displaying random phase screens generated through the Kolmogorov model of turbulence on the DMD [17]. The Kolmogorov phase screen is given by $\Phi = \mathrm{Re}\left(\mathcal{F}^{-1}(\mathbb{M}\sqrt{\phi})\right)$, where $\mathbb{M}$ is the encoded random matrix, and the approximated power spectral density $\phi \approx 0.023 r_0^{-\frac{5}{3}} f^{-\frac{11}{3}}$. Here, $\mathrm{Re}(z)$ indicates the real part of a complex number z, $\mathcal{F}^{-1}$ is the inverse Fourier transform, and f is the spatial frequency of the light field. Particularly, the

encoding of Kolmogorov phase screens in a DMD is achieved through amplitude-only spatial light modulation. These generated Kolmogorov phase screens are encoded into a video at a rate of 60 frames per second and displayed on the DMD. Another 4-f system and an iris are used to filter the first diffraction order of the beam reflected off the DMD.

Experimental setup and measurements

In order to project our system into two separate OAM modes, we first divide the beam from the DMD in two with a 50:50 beam splitter. These beams illuminate two angular double-slits on two spatial light modulators (SLMs) [24]. The SLMs are also used to display phase holograms which induce a shift in the beams' OAM spectra. Specifically, if we are interested in measuring the OAM ℓ in arm one, then we will shift that arm's OAM spectrum by $-\ell$. This produces a beam with a new OAM distribution such that its Gaussian mode occurs with the same frequency as the ℓ mode of the initial beam. These shifted beams are then coupled into two single-mode fibers (whose fundamental modes are Gaussian). This process of shifting the OAM spectrum and then coupling into single-mode fibers constitutes our protocol for OAM projection [44]. These fibers then direct photons to two superconducting nanowire single-photon detectors (SNSPDs) that perform photon number resolving (PNR) detection [14, 19, 20].

Implementation of photon-number-resolving detection

In order to perform PNR detection with our SNSPDs, we use the surjective photon counting method described in Refs. [19, 45]. Specifically, the photons are detected by the SNSPDs and then recorded by a time tagger. The collected data is then divided into time bins of 1 μs, which corresponds to the coherence time of our CW laser. Since the dead time of our SNSPDs is small compared to the length of the time bin, the measurements are guaranteed to be in a single-temporal-mode field. Finally, the number of events in each time bin are counted to retrieve photon number statistics.

Supplementary Information

The online version contains supplementary material available at https://doi.org/10.1186/s43074-024-00153-4.

Supplementary Material 1.

Acknowledgements
We thank Dr. Ivan Agullo and Dr. Javier Sanchez-Mondragon for discussions.

Authors' contributions
The experiment was designed by C.Y., M.H., and O.S.M.L. The theoretical description was developed by R.B.D., C.Y., R.J.L-M., and O.S.M.L. The experiment was performed by M.H., C.Y., F.M., and J.F. The data was analysed by R.B.D., C.Y. and O.S.M.L. The project was supervised by C.Y. and O.S.M.L. The idea was conceived by O.S.M.L and C.Y. All authors contributed to the writing of the paper and approved the final version of the paper.

Funding
C. Y., F.M., J. F., and O. S. M. L. acknowledge support from the Army Research Office (ARO), through the Early Career Program (ECP) under the grant no. W911NF-22-1-0088. M. H. and O. S. M. L. thank the U.S. Department of Energy (DOE), Office of Science (SC), for supporting this research through the Program of Nuclear Physics under the NP-QIS grant: DE-SC0023694. Also, R. B. D. and O. S. M. L. acknowledge funding from the National Science Foundation through Grant No. OMA 2231387. R.J.L.-M. thankfully acknowledges financial support by DGAPA-UNAM under the project UNAM-PAPIIT IN101623.

Data availability
The data sets generated and/or analyzed during this study are available from the corresponding author or last author on reasonable request.

Declarations

Competing interests
The authors declare no competing interests.

Received: 27 August 2024 Revised: 10 November 2024 Accepted: 20 November 2024
Published online: 27 November 2024

References

1. Zurek WH. Decoherence and the Transition from Quantum to Classical. Phys Today. 1991;44(10):36–44. https://doi.org/10.1063/1.881293.
2. De Martini F, Sciarrino F. Colloquium: Multiparticle quantum superpositions and the quantum-to-classical transition. Rev Mod Phys. 2012;84:1765–89. https://doi.org/10.1103/RevModPhys.84.1765.
3. Arndt M, Hornberger K. Testing the limits of quantum mechanical superpositions. Nat Phys. 2014;10(4):271–7. https://doi.org/10.1038/nphys2863.
4. Vedral V. Quantifying entanglement in macroscopic systems. Nature. 2008;453(7198):1004–7. https://doi.org/10.1038/nature07124.
5. Gerlich S, Eibenberger S, Tomandl M, Nimmrichter S, Hornberger K, Fagan PJ, et al. Quantum interference of large organic molecules. Nat Commun. 2011;2(1):263. https://doi.org/10.1038/ncomms1263.
6. Fein YY, Geyer P, Zwick P, Kiałka F, Pedalino S, Mayor M, et al. Quantum superposition of molecules beyond 25 kDa. Nat Phys. 2019;15(12):1242–5. https://doi.org/10.1038/s41567-019-0663-9.
7. Dittel C, Dufour G, Weihs G, Buchleitner A. Wave-Particle Duality of Many-Body Quantum States. Phys Rev X. 2021;11:031041. https://doi.org/10.1103/PhysRevX.11.031041.
8. Lvovsky AI, Ghobadi R, Chandra A, Prasad AS, Simon C. Observation of micro-macro entanglement of light. Nat Phys. 2013;9(9):541–4. https://doi.org/10.1038/nphys2682.
9. Bouganne R, Bosch Aguilera M, Ghermaoui A, Beugnon J, Gerbier F. Anomalous decay of coherence in a dissipative many-body system. Nat Phys. 2020;16(1):21–5. https://doi.org/10.1038/s41567-019-0678-2.
10. Aspuru-Guzik A, Walther P. Photonic quantum simulators. Nat Phys. 2012;8(4):285–91. https://doi.org/10.1038/nphys2253.
11. You C, Miller A, León-Montiel RDJ, Magaña-Loaiza OS. Multiphoton quantum van Cittert-Zernike theorem. npj Quantum Inf. 2023;9(1):50. https://doi.org/10.1038/s41534-023-00720-w.
12. Dell'Anno F, Siena SD, Illuminati F. Multiphoton quantum optics and quantum state engineering. Phys Rep. 2006;428:53–108. https://doi.org/10.1016/j.physrep.2006.01.004.
13. Fröwis F, Sekatski P, Dür W, Gisin N, Sangouard N. Macroscopic quantum states: Measures, fragility, and implementations. Rev Mod Phys. 2018;90:025004. https://doi.org/10.1103/RevModPhys.90.025004.
14. Magaña-Loaiza OS, León-Montiel RDJ, Perez-Leija A, U'Ren AB, You C, Busch K, et al. Multiphoton quantum-state engineering using conditional measurements. npj Quantum Inf. 2019;5(1):80. https://doi.org/10.1038/s41534-019-0195-2.
15. Harder G, Bartley TJ, Lita AE, Nam SW, Gerrits T, Silberhorn C. Single-Mode Parametric-Down-Conversion States with 50 Photons as a Source for Mesoscopic Quantum Optics. Phys Rev Lett. 2016;116:143601. https://doi.org/10.1103/PhysRevLett.116.143601.
16. Smith TA, Shih Y. Turbulence-Free Double-slit Interferometer. Phys Rev Lett. 2018;120:063606. https://doi.org/10.1103/PhysRevLett.120.063606.
17. Hong M, Miller A, León-Montiel RDJ, You C, Magaña-Loaiza OS. Engineering Super-Poissonian Photon Statistics of Spatial Light Modes. Laser Photon Rev. 2023;17(10):2300117. https://doi.org/10.1002/lpor.202300117.
18. Gatti A, Brambilla E, Lugiato LA. Entangled Imaging and Wave-Particle Duality: From the Microscopic to the Macroscopic Realm. Phys Rev Lett. 2003;90:133603. https://doi.org/10.1103/PhysRevLett.90.133603.
19. You C, Quiroz-Juárez MA, Lambert A, Bhusal N, Dong C, Perez-Leija A, et al. Identification of light sources using machine learning. Appl Phys Rev. 2020;7(2):021404. https://doi.org/10.1063/1.5133846.
20. You C, Hong M, Bierhorst P, Lita AE, Glancy S, Kolthammer S, et al. Scalable multiphoton quantum metrology with neither pre- nor post-selected measurements. Appl Phys Rev. 2021;8(4):041406. https://doi.org/10.1063/5.0063294.
21. Berry MV. Disruption of wavefronts: statistics of dislocations in incoherent Gaussian random waves. J Phys A Math Gen. 1978;11(1):27. https://doi.org/10.1088/0305-4470/11/1/007.
22. Dennis MR, O'Holleran K, Padgett MJ. Chapter 5 Singular Optics: Optical Vortices and Polarization Singularities. vol. 53 of Progress in Optics. Elsevier; 2009. pp. 293–363. https://doi.org/10.1016/S0079-6638(08)00205-9.
23. Gbur GJ. Singular optics. Boca Raton: CRC Press; 2016.
24. Magaña-Loaiza OS, Mirhosseini M, Cross RM, Rafsanjani SMH, Boyd RW. Hanbury Brown and Twiss interferometry with twisted light. Sci Adv. 2016;2(4):e1501143. https://doi.org/10.1126/sciadv.1501143.
25. Jeltes T, McNamara JM, Hogervorst W, Vassen W, Krachmalnicoff V, Schellekens M, et al. Comparison of the Hanbury Brown-Twiss effect for bosons and fermions. Nature. 2007;445(7126):402–5. https://doi.org/10.1038/nature05513.
26. Mostafavi F, Hong M, Dawkins RB, Ferdous J, Jin RB, León-Montiel RDJ, et al. Multiphoton Quantum Imaging using Natural Light. arXiv preprint arXiv:240512794. 2024.
27. Wubs M. Multiphoton quantum statistics from scattered classical light. Nat Phys. 2024;20(5):689–90. https://doi.org/10.1038/s41567-024-02447-7.
28. Branderhorst MPA, Londero P, Wasylczyk P, Brif C, Kosut RL, Rabitz H, et al. Coherent Control of Decoherence. Science. 2008;320(5876):638–43. https://doi.org/10.1126/science.1154576.
29. Yu T, Eberly JH. Sudden Death of Entanglement. Science. 2009;323(5914):598–601. https://doi.org/10.1126/science.1167343.

30. Bender N, Sun M, Yilmaz H, Bewersdorf J, Cao H. Circumventing the optical diffraction limit with customized speckles. Optica. 2021;8(2):122–9. https://doi.org/10.1364/OPTICA.411007.
31. Nye JF, Berry MV. Dislocations in wave trains. Proc R Soc Lond A Math Phys Sci. 1974;336(1605):165–90. https://doi.org/10.1098/rspa.1974.0012.
32. Wright KC, Leslie LS, Hansen A, Bigelow NP. Sculpting the Vortex State of a Spinor BEC. Phys Rev Lett. 2009;102:030405. https://doi.org/10.1103/PhysRevLett.102.030405.
33. Glauber RJ. Coherent and Incoherent States of the Radiation Field. Phys Rev. 1963;131:2766–88. https://doi.org/10.1103/PhysRev.131.2766.
34. Mandel L, Wolf E. Optical Coherence and Quantum Optics. Cambridge University Press; 1995. https://doi.org/10.1017/CBO9781139644105.
35. Dawkins RB, Hong M, You C, Magaña-Loaiza OS. The quantum Gaussian-Schell model: a link between classical and quantum optics. Opt Lett. 2024;49(15):4242–5. https://doi.org/10.1364/OL.520444.
36. Malý P, Lüttig J, Rose PA, Turkin A, Lambert C, Krich JJ, et al. Separating single- from multi-particle dynamics in nonlinear spectroscopy. Nature. 2023;616(7956):280–7. https://doi.org/10.1038/s41586-023-05846-7.
37. Jaeger G. What in the (quantum) world is macroscopic? Am J Phys. 2014;82(9):896–905. https://doi.org/10.1119/1.4878358.
38. Hong M, Dawkins RB, Bertoni B, You C, Magaña-Loaiza OS. Nonclassical near-field dynamics of surface plasmons. Nat Phys. 2024;20(5):830–5. https://doi.org/10.1038/s41567-024-02426-y.
39. Hiekkamäki M, Bouchard F, Fickler R. Photonic Angular Superresolution Using Twisted N00N States. Phys Rev Lett. 2021;127:263601. https://doi.org/10.1103/PhysRevLett.127.263601.
40. Jha AK, Leach J, Jack B, Franke-Arnold S, Barnett SM, Boyd RW, et al. Angular Two-Photon Interference and Angular Two-Qubit States. Phys Rev Lett. 2010;104:010501. https://doi.org/10.1103/PhysRevLett.104.010501.
41. Mair A, Vaziri A, Weihs G, Zeilinger A. Entanglement of the orbital angular momentum states of photons. Nature. 2001;412(6844):313–6. https://doi.org/10.1038/35085529.
42. Georgescu IM, Ashhab S, Nori F. Quantum simulation. Rev Mod Phys. 2014;86:153–85. https://doi.org/10.1103/RevModPhys.86.153.
43. Zhang Z, You C, Magaña-Loaiza OS, Fickler R, León-Montiel RDJ, Torres JP, et al. Entanglement-based quantum information technology: a tutorial. Adv Opt Photon. 2024;16(1):60–162. https://doi.org/10.1364/AOP.497143.
44. Magaña-Loaiza OS, Boyd RW. Quantum imaging and information. Rep Prog Phys. 2019;82(12):124401. https://doi.org/10.1088/1361-6633/ab5005.
45. Rafsanjani SMH, Mirhosseini M, Magaña-Loaiza OS, Gard BT, Birrittella R, Koltenbah BE, et al. Quantum-enhanced interferometry with weak thermal light. Optica. 2017;4(4):487–91. https://doi.org/10.1364/OPTICA.4.000487.

Publisher's Note